

Structural Association of Nonsteroidal Anti-Inflammatory Drugs with Lipid Membranes

Mohan Babu Boggara,^{†,||} Mihaela Mihailescu,^{‡,§} and Ramanan Krishnamoorti^{*,†}

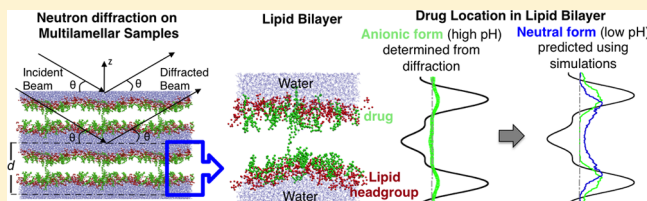
[†]Department of Chemical and Biomolecular Engineering, University of Houston, Houston, Texas 77204, United States

[‡]Institute for Bioscience and Biotechnology Research, University of Maryland, Rockville, Maryland 20850, United States

[§]National Institute for Standard and Technology, Center for Neutron Research, Gaithersburg, Maryland 20899, United States

Supporting Information

ABSTRACT: The location and distribution of ibuprofen, a model nonsteroidal anti-inflammatory drug, in a phospholipid bilayer was examined in molecular detail by a combination of neutron diffraction and computer simulations. In addition to their use as antipyretic, analgesic, and anti-inflammatory drugs, such nonsteroidal anti-inflammatory drugs are used in the treatment of a number of diseases including cancer and Alzheimer's. As a side effect, they have been known to cause gastrointestinal toxicity, although the molecular mechanism of their action is poorly understood. In this study, we have used contrast variation-based neutron diffraction to determine the position of the drug in a 1,2-dioleoyl-*sn*-glycero-3-phosphatidylcholine lipid bilayer and explore changes to the bilayer structure upon drug incorporation. In its charged state, the drug was found to locate in the polar headgroup region of the phospholipid bilayer, to induce bilayer thinning, and to increase the number of water molecules closely associated with the bilayer. These structural insights are consistent with molecular dynamics simulations and earlier macroscopic experiments of vesicle structure and dynamics. Using MD simulations, the neutral ibuprofen, typically observed at low pH and inaccessible to the diffraction studies, was found to locate deeper within the bilayer than the charged form.



INTRODUCTION

Nonsteroidal anti-inflammatory drugs (NSAIDs) are widely used for their antipyretic, analgesic, and anti-inflammatory action¹ and have also been implicated in the treatment of other diseases including cancer² and Alzheimer's.³ Long-term use of NSAIDs results in gastrointestinal (GI) toxicity and mild to sometimes fatal ulcers.⁴ Various mechanisms on how NSAIDs cause GI toxicity have been proposed including inhibition of membrane active cyclooxygenase (COX), mucosal blood flow reduction, or direct topical interaction with the membranes that line the GI tract.^{1,5–7} NSAIDs have also been shown to affect clustering in model membranes as well as cell membranes,⁸ and that study suggests that NSAIDs might act either directly by interacting with the related membrane active proteins or indirectly via altering biophysical properties of the membranes.

The amphiphilic nature of NSAIDs and their pH-dependent charge state (with pK_a values in the physiological pH range⁹) render them as strong candidates to interact with either the apolar hydrocarbon chains or the polar headgroup moieties of lipid membranes and alter the biophysical properties of membranes.¹⁰ For the same reasons, it is more challenging to understand the partitioning behavior of NSAIDs in membranes as compared to simple hydrophobic molecules. To understand the molecular origins of the partitioning, it is also necessary to determine how NSAIDs are distributed within the lipid bilayer membranes at subnanometer resolution. More importantly, the pH in the GI tract varies from ~ 2 in the stomach to ~ 8 in the

large intestine,⁹ making it important to understand the drug distribution at both low and high pH values. Neutron diffraction, which exploits the large difference between the coherent scattering amplitude of hydrogen ($b_H = -3.374 \times 10^{-12}$ cm) and deuterium ($b_D = 6.65 \times 10^{-12}$ cm), provides a sensitive method of isomorphous H/D replacement, which can be used to locate individual atoms or molecular groups, with sub-angstrom accuracy.¹¹ Our previous studies using MD simulations and neutron scattering measurements suggested that NSAIDs partition into model lipid membranes at all pH values and affect a number of bilayer properties including thickness, headgroup hydration, and the bending modulus.^{12–14} Other studies probing NSAID–membrane systems at a molecular level include partitioning and location of NSAIDs in the membrane using fluorescence spectroscopy techniques,¹⁵ pH-dependent fusion of vesicles induced by oxicam class of NSAIDs,¹⁶ and animal studies suggesting cytotoxicity caused by increased membrane permeability due to NSAID interactions.¹⁷ Also, several studies used liposomes as model systems to study the effect of NSAIDs on the structural properties of lipid bilayers.^{18–27} Those studies provide valuable insights about NSAID–membrane interactions, typically relying either on probes that might perturb the membranes or on the accurate

Received: July 2, 2012

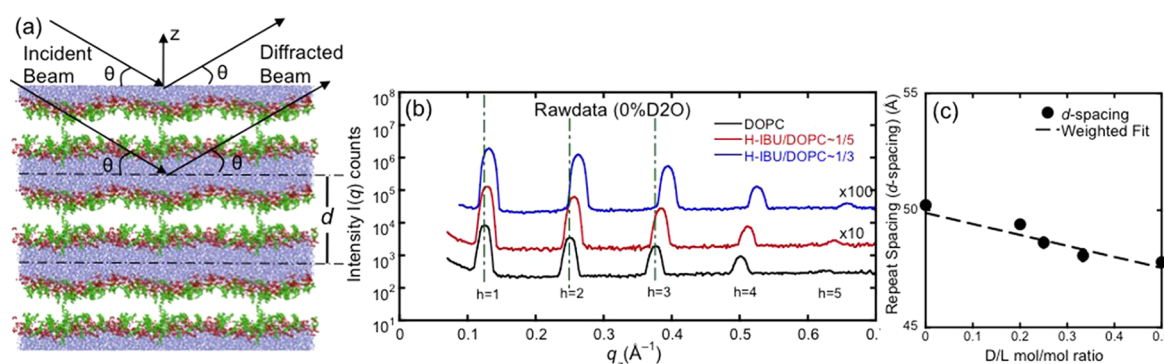


Figure 1. Raw neutron diffraction data from a multilamellar lipid sample and Bragg d -spacing obtained from the diffraction data. (a) Representation of multilamellar lipid sample used for diffraction. Heavy headgroup atoms (P, N, and O) are shown in red, drug molecules are shown in green, and water is shown in blue. Lipid tails are not shown for clarity. (b) Diffraction data for DOPC and ibuprofen/DOPC at D/L \approx 1/5 and \approx 1/3. Peaks in the DOPC data are marked with a dashed line to indicate that peaks shift to the right and the distance between peaks increases as the D/L ratio is increased. (c) Bragg d -spacing obtained from the distance between peaks of the multilamellar system is shown as a function of D/L ratio (errors are smaller than the size of the symbols used).

knowledge of the location of these probes and are of somewhat low resolution (e.g., liposome-based models).

In this study, we used neutron diffraction along with atomistic MD simulations to examine the organization of ibuprofen (a model NSAID), lipid, and water molecules in a fluid bilayer membrane composed of 1,2-dioleoyl-*sn*-glycero-3-phosphatidylcholine (DOPC). One-dimensional density profiles, along the normal to the bilayer, were calculated from neutron diffraction from lamellar stacks of bilayers hydrated from the vapor phase, for a series of drug/lipid (D/L) molar ratios: D/L = 0, 1/5, 1/4, 1/3, and 1/2. We have exploited hydrogen to deuterium isotopic substitution to specifically determine the drug and water distribution, as well as the water content of the lipid membrane. We have addressed further inquiries into the molecular details of the drug–lipid interaction by all-atom MD simulations, using neutron data as a basis for model validation. Because the pK_a of single carboxylic acid group of ibuprofen is ~ 5.2 ,⁹ the drug exists in anionic form at neutral pH ($\text{pH} \gg pK_a$) due to deprotonated carboxylic acid and in uncharged form at acidic pH ($\text{pH} \ll pK_a$). In the experiments, neutral pH was maintained rendering the drug to be primarily in its anionic form. The one-dimensional neutron profiles were compared to simulated profiles of the bilayer/drug system under conditions that mimic the experiment. MD simulations were then used to extend the predictions to the uncharged form of the drug typically observed under physiologically important acidic pH conditions.

RESULTS

1. Diffraction Data. Diffraction data along the ($h, 0, 0$) direction were collected for multilamellar samples, hydrated at 86% relative humidity from the vapor phase of a saturated salt (KCl) solution and at 23 °C. Fluid phase lipid multilayers inherently form less-ordered structure, due to high thermal disorder, leading to the observation of only ~ 5 – 8 diffraction peaks.²⁸ We observed five statistically significant orders of diffraction for the multilamellar lipid samples investigated (Figure 1a). The systematic shift to higher angle (equivalently q) in the position of the Bragg peaks (Figure 1b) with increasing molar fraction of the drug indicates a decrease in the Bragg repeat spacing (d), that is, the repeating unit dimension (bilayer thickness + associated water of hydration). The relative position of the peaks was used to determine the repeat spacing

($d = 2\pi/(q_{h+1} - q_h)$). With increased drug to lipid mole ratios (denoted here as D/L), the Bragg d -spacing is reduced from 50.2 ± 0.2 Å (error reported here is 3 times the standard deviation of the measurements) for pure DOPC to 47.8 ± 0.2 Å for D/L of 1/2 (Figure 1c), following a roughly linear dependence on the added ibuprofen. We have earlier observed a similar bilayer thinning effect of ibuprofen on DMPC lipid bilayers using elastic small-angle neutron scattering studies (SANS) on small unilamellar vesicles.¹³

2. Bilayer Structure. For drug and water distributions, the diffraction data are translated, by a Fourier synthesis (see Materials and Methods), into the scattering length density (SLD) of the bilayer along the z -axis^{11,29,30} and allow us to delineate structural information in the bilayer. To determine the SLD profiles, we have adopted an absolute-relative scale representation introduced by Wiener and White,^{28,31,32} where the amplitude of the scattering length of the lipid along the z -axis is determined up to a constant (S) accounting for the area per lipid. For DOPC membranes, the SLD profile accounts for the unit cell made up of lipid and the associated water. When the drug is present, the SLD calculation takes into account the composition of the unit cell (drug, lipid, and associated water, contributing in proportion to their molar fractions). The procedure to determine the SLD on absolute scale is described briefly in the Materials and Methods section and detailed in earlier works.^{28,31,33–35}

Hydrogen to deuterium substitution in either the salt solution used for hydration (H_2O to D_2O) or the methyl group of the ibuprofen ($-\text{CH}_3$ to $-\text{CD}_3$) allows one to contrast variation relative to their protonated forms. Water and drug distributions are determined directly by deuterium difference (i.e., by subtracting the profile of the protonated sample, measured in H_2O from the profiles of the two deuterated forms: containing deuterated water or deuterated drug, respectively) (Figure 2a). The drug distribution is symmetric in the two leaflets of the bilayer and can be described by a single Gaussian function, while the water distribution in the interbilayer space is best described by a sum of two Gaussian functions. The fitted parameters for water and drug distribution are given in Table 1.

a. Effect of Ibuprofen on Bilayer Structure. The scattering length density across the lipid bilayer exhibits two prominent peaks. These peaks correspond to the carbonyl groups and the

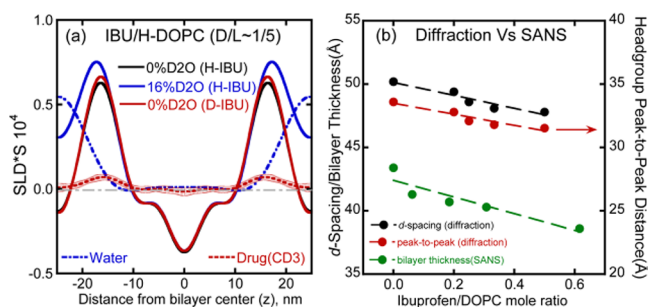


Figure 2. Scattering length density (SLD) profiles on absolute (per lipid) scale showing details of the bilayer structure and the bilayer thickness derived from SLD. (a) SLD profiles are shown for the ibuprofen/DOPC system at $D/L \approx 1/5$. The data shown are for the H-IBU/DOPC hydrated with 0% D_2O (black) and 16% D_2O (blue) water, as well as for D-IBU/DOPC hydrated with 0% D_2O (red). Also shown are the water (blue-dashed) and drug distribution (α -CD₃, red-dashed). (b) Bragg d -spacing and peak-to-peak distance derived from SLD profiles (based on the data for 0% D_2O) are shown as a function of D/L ratios. Bilayer thickness previously obtained using small-angle neutron scattering¹³ (green) for ibuprofen–DMPC systems is also shown for comparison.

oxygen atoms of the glyceryl–fatty acid ester bonds that flank the hydrocarbon region (Figure 2a). We therefore estimate the thickness of the hydrocarbon region from the distance between carbonyl groups, d_{pp} (peak-to-peak), across the bilayer as reported in Figure 2b. Both the repeat d -spacing and the distance between carbonyl groups (d_{pp}) show a linear decrease: going from $D/L = 0$ to $1/2$, the net decrease in d -spacing is 2.4 ± 0.2 and $\approx 2.1 \pm 0.3$ Å in d_{pp} (Figure 2b). This indicates that the observed decrease in the repeat spacing is primarily due to the thinning of the bilayer when the drug is present. Moreover, these results also indicate that the combined thickness of the headgroup, the associated water molecules, and the interlamellar water layer remains unaffected by the addition of the drug.

b. Drug Distribution. The distribution of ibuprofen in the bilayer was determined from the deuterium difference, using a deuterium-labeled methyl group (α -CD₃) of the drug. Analysis of the deuterium distribution in terms of a single Gaussian function provided the values for its mean position (Z_{drug}), and $1/e$ half-width (A_{drug}). While the width of the drug distribution is constant within experimental error, the mean position was found to shift little in the range of ± 15.3 – 15.9 (± 0.2) Å from the bilayer center, over the range of D/L ratios studied (Figure 3). The deuterium peak of the drug is proximal to the peak associated with the lipid carbonyls in the SLD profiles for the bilayer. This indicates that the drug, in its anionic charged state, resides at the interface between the lipid polar headgroup and hydrocarbon regions consistent with observations from our

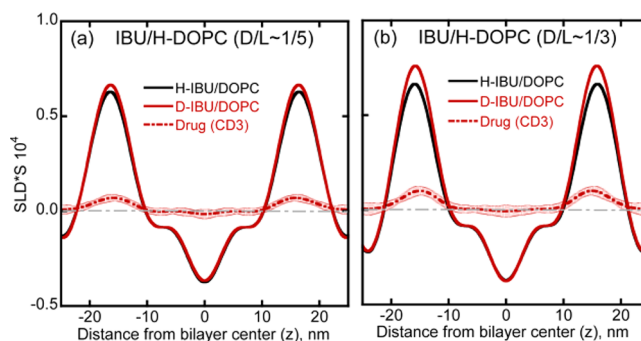


Figure 3. Distribution of ibuprofen (charged form) in the DOPC bilayer with SLD profiles for H-IBU/DOPC (0% D_2O , black) and D-IBU/DOPC (0% D_2O , red) shown as reference. Distribution of ibuprofen at $D/L \approx 1/5$ ratio and $\approx 1/3$ ratio are shown in panels (a) and (b), respectively. Uncertainties in the drug distribution profiles were obtained using Monte Carlo error analysis (see Materials and Methods).

earlier free energy predictions for similar NSAID–lipid systems¹⁴ as well as studies in the literature on other NSAIDs.¹⁵ The location of the drug relative to the lipid carbonyl remains broadly unchanged, within experimental error, with increasing drug concentration. The linear decrease in the bilayer thickness with addition of drug up to a D/L ratio of $1/2$ and the almost unchanged profile of the drug distribution suggest that a significant amount of drug can be incorporated into the lipid without any evidence of phase separation.

c. Effect of Ibuprofen on Bilayer Hydration. The profile of the interbilayer water distribution found by the deuterium difference analysis of the Fourier coefficients ($F_{D_2O}(h) - F_{H_2O}(h)$) is best described by a sum of two Gaussian functions (Table 1). The positions (Z_{water}) and $1/e$ half-width (A_{water}) of these distributions are given in Table 1. With increasing drug concentration in the membrane, changes in A_{water} are small, while the position of the water peak shifts toward the bilayer center, mirroring the changes in the position of the carbonyl groups relative to the bilayer center (Figure 4a). This is probably due to the fact that most of the water present in the lipid membranes at partial hydration (here, 86% relative humidity (RH)) is tightly associated with the phosphate–carbonyl groups of the lipid via hydrogen bonds and dipolar interactions. The number of water molecules associated with one phosphatidylcholine headgroup, at 86% RH, was determined to be 7.7, by gravimetric measurements for DOPC.³³ For the cases where the ibuprofen is added to the DOPC membrane, N_w was determined by calibrating the amplitude of the Fourier profiles, including water peaks, using isotopically substituted ibuprofen ($-\text{CD}_3$) data to calibrate the scale (see Materials and Methods). As shown in Figure 4b, N_w

Table 1. Fitted Parameters for Drug and Water Distributions^a

drug/lipid (D/L) molar ratio	d -spacing (Å)	drug distribution		water distribution		
		Z_{drug} (Å)	A_{drug} (Å) ($\sqrt{2}\sigma_{drug}$)	waters per lipid (N_w)	Z_{water} (Å)	A_{water} (Å) ($\sqrt{2}\sigma_{drug}$)
0	50.2 ± 0.1	n.a.	n.a.	7.7^b	22.70 ± 0.41	6.50 ± 0.49
1/5	49.4 ± 0.1	15.89 ± 0.17	4.51 ± 0.26	8.1	22.08 ± 0.29	5.74 ± 0.45
1/4	48.6 ± 0.2	n.d.	n.d.	n.d.	n.d.	n.d.
1/3	48.1 ± 0.2	15.27 ± 0.08	4.40 ± 0.12	8.5	21.28 ± 0.23	5.27 ± 0.36
1/2	47.8 ± 0.2	n.d.	n.d.	n.d.	n.d.	n.d.

^aData collected at 86% relative humidity and 23 °C. n.a., not applicable; n.d., not determined. ^bHristova and White, 1998.²³

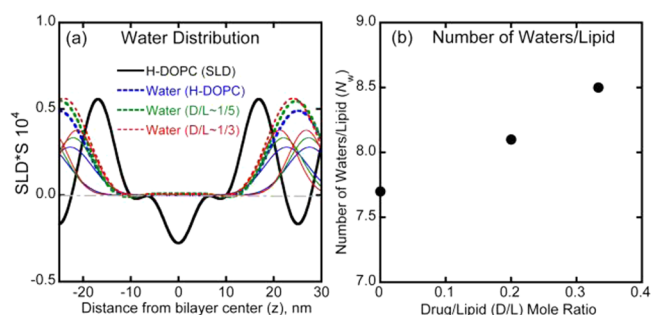


Figure 4. Distribution of water between the bilayers and number of waters/lipid estimated from such distributions. (a) Distribution of water between the bilayers for DOPC (blue-dashed) and ibuprofen/DOPC systems at D/L ratios of $\approx 1/5$ (green-dashed) and $\approx 1/3$ (red-dashed). The water layer shown as dashed lines is the sum of two water layers (shown as thin lines of same color as dashed) that belong to the two opposing bilayers. A part of the second bilayer is shown on the right side to highlight this feature. SLD profile for DOPC is shown as reference. (b) Number of waters/lipid (N_w) as a function of D/L ratio.

increases with increasing drug molar fraction, that is, D/L ratio. The observed increase in N_w with increase in D/L ratio amounts to ≈ 2 – 2.4 water molecules for every single drug molecule added to the unit cell.

3. Comparison to Molecular Dynamics Simulations.

We performed all-atom MD simulations of a pure DOPC bilayer and for bilayers incorporating either the anionic charged or the uncharged forms of ibuprofen at D/L ratios of 1/4 and 1/2. MD simulations were performed using GROMACS software³⁶ with *ffgmx* forcefield³⁷ as implemented in GROMACS. Using a model bilayer made of 128 DOPC molecules and 4789 water molecules, constant pressure (1 bar) and temperature (323 K) simulations (NPT) with periodic boundary conditions were performed for a total of 35 ns (see Materials and Methods for details). The drug was modeled using PRODRG server³⁸ where the charged drug was treated as carrying a net charge of -1 . Because all of the molecular motions in the investigated drug–lipid system occur on time scales of a few picoseconds, atomistic MD simulations run over multianoseconds after equilibration are considered to be good representations of the equilibrium structures measured in the diffraction experiments that represent time and ensemble averages. In these simulations, after allowing for system equilibration of 15 ns, the analysis was performed on trajectories averaged over the last 20 ns of simulation time to

obtain spatial distribution and SLD profiles of different molecular groups for direct comparison with diffraction experiments. The overall bilayer structure in the presence of the charged ibuprofen predicted by simulations is in reasonable agreement with the neutron diffraction results (Figure 5a). In addition, both the position of the drug and its spatial distribution predicted by simulations agree well with experiments (Figure 5b).

To further explore the distribution of ibuprofen in its uncharged state (i.e., carboxylic acid is protonated and representative of the behavior at low pH values), we simulated DOPC bilayers containing uncharged forms of ibuprofen at D/L ratios of 1/4 and 1/2. In this case, the drug was modeled using PRODRG to carry a net charge of 0, while the other conditions for the simulations remained the same as described above. MD-based distributions of the drug in charged and uncharged forms are compared in Figure 5c. To better represent the heterogeneity of the bilayer along the normal (from the bilayer center extending up to the center of interlamellar), bilayers are typically modeled to have four regions.³⁹ According to this four-region model, ≈ 6 Å on either side of the bilayer center is considered to be low-density tail region, ≈ 6 – 13 Å from the bilayer center is the high-density tail region, ≈ 13 – 20 Å from the bilayer center is high-density headgroup region, and ≈ 20 – 27 Å from the bilayer center is low-density headgroup region. Figure 5c shows that both forms of the drug tend to distribute significantly into the high-density regions of the bilayer (Figure 6). The peak location of the drug

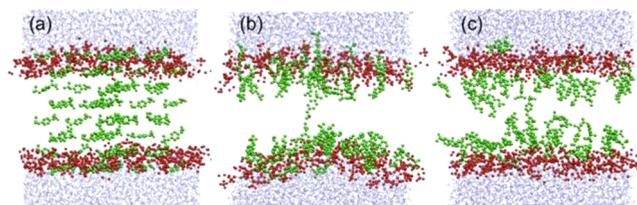


Figure 6. Snapshots from MD simulations for the system containing 64 ibuprofen molecules in a bilayer made of 128 DOPC lipid molecules (D/L $\approx 1/2$). Drug molecules are colored green, heavy atoms (P, N, and O) of the lipid headgroup are colored red, and water is colored light blue. Lipid tails are not shown for clarity. (a) Structure of the bilayer with drug molecules at 0 ns. (b) Equilibrated structure of the bilayer containing charged form of ibuprofen. (c) Equilibrated structure of the bilayer containing neutral form of ibuprofen.

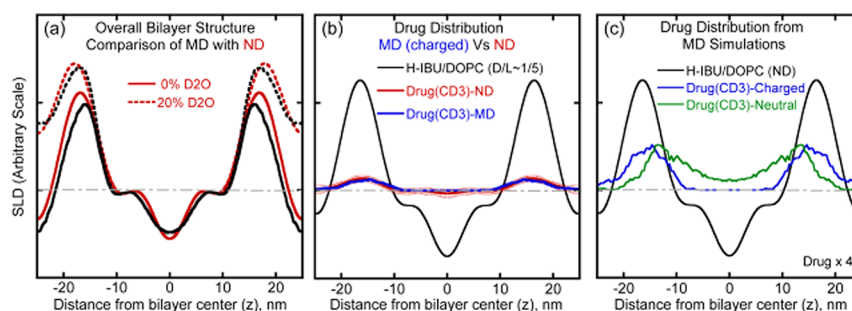


Figure 5. Comparison between MD simulations and neutron diffraction (ND) for bilayer structure and drug distribution. (a) Comparison of SLD profiles for DOPC at 0 and 20% D₂O. (b) Comparison of the drug distribution (α -CD3) between MD (D/L $\approx 1/4$) and ND (D/L $\approx 1/5$). The red band shows the extent of the experimental uncertainty in the drug profile. (c) Distributions of deuterated ibuprofen (α -CD3) in neutral and charged forms predicted from MD simulations.

in its charged form is in the headgroup region, while that of the uncharged form is slightly shifted (≈ 2 Å shift) toward the center of the bilayer.

The reasonable agreement found between the neutron diffraction data and MD simulations prompted further exploration into the atomistic details of the drug–membrane interactions offered exclusively by MD. First, interactions of water with various molecular groups such as lipid headgroup moieties (choline, phosphate, and carbonyls) and drug carboxylic group were probed by calculating radial distribution functions (RDF) between different molecular moieties. The RDF between two molecular groups represents the probability of finding the second group as a function of distance from the center of first group. Comparison of RDF calculated between the lipid carbonyls and water for DOPC with that of D/L $\approx 1/4$ suggests that there is minimal effect on the hydration of lipid headgroup due to the addition of the drug (Figure 7a and

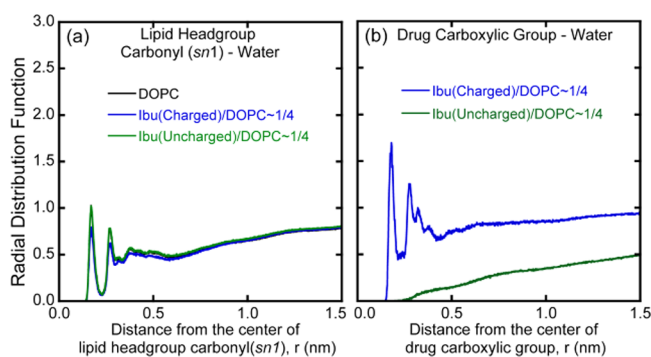


Figure 7. Radial distribution functions (RDF) between different moieties calculated from MD simulations. (a) RDF between the lipid headgroup carbonyl (*sn1*) and water compared between DOPC and ibuprofen/DOPC at D/L $\approx 1/4$. (b) RDF between the drug carboxylic group (in charged and uncharged forms) and water for the system at D/L $\approx 1/4$.

Supporting Information S2). On the other hand, RDF between the drug carboxylic group (in charged form) and water (Figure 7b) shows strong peaks, suggesting that the drug is significantly hydrated within the bilayer. Water association with the drug in its charged form is due to the formation of a significant number of hydrogen bonds between the drug and water (estimated to be ≈ 120 per time frame in the case of D/L $\approx 1/4$). However, when the drug is in uncharged form, the RDF profiles lack any strong peaks and are consistent with the absence of hydrogen bonding between the two moieties.

Last, we note from the analysis of the MD simulations that the drug–lipid interaction is not likely to be dipole–dipole in origin as the lipid P–N vector orientation, a sensitive measure of changes in the dipolar interactions of the lipid, is unaffected by the addition of the charged or uncharged drug (Supporting Information S3). Moreover, we note that the drug, irrespective of charge state, is predominantly oriented parallel to the bilayer normal with its carboxylic group toward the lipid headgroup and with its aromatic group oriented toward the hydrocarbon chains (Supporting Information S4).

To elucidate the possible reason for the membrane thinning effect of ibuprofen, we plotted the distance between headgroup atoms (phosphate and the choline) of the two monolayers for DOPC and compared it to that for the ibuprofen/DOPC system in both charged and neutral forms of ibuprofen. The comparison is shown in Figure 8.

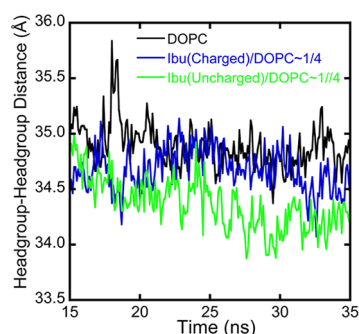


Figure 8. Distance between the headgroup atoms (phosphate and choline) of the two monolayers calculated from MD simulations for DOPC (black), ibuprofen(charged)/DOPC at D/L $\approx 1/4$ (blue), and ibuprofen(uncharged)/DOPC at D/L $\approx 1/4$ (green).

DISCUSSION

The amphiphilic nature of most NSAIDs, with some exhibiting multiple charge states depending on microenvironment,⁴⁰ makes it challenging to understand their interactions with, and partitioning into, lipid membranes.^{15–17,40} Using fluorescence techniques, NSAIDs have been located either in the headgroup/chain interface when the drug is charged¹⁵ or in the bilayer interior when the drug is uncharged.⁴¹ The main advantage offered by neutron diffraction is that we can determine the drug location accurately by isomorphous replacement of hydrogen with deuterium. Replacing H with D, in comparison to having large molecular tags as labels, is less likely to interfere with the native interactions between drug and lipid bilayer system. We have shown that, at neutral pH, the charged form of the drug is distributed in the interfacial region, in a fairly narrow range around the position of the lipid carbonyl groups. This is consistent with previous literature using labeled systems as well as our earlier free energy calculations and macroscale studies.^{13,14}

One of the significant effects of ibuprofen on the bilayer structure is that of membrane thinning. Studies in the literature on number of membrane active molecules suggest that the net effect of such molecules on the membrane thickness is modulated by their size, anisotropy, and rigidity. Cholesterol being large, anisotropic, and rigid with a polar hydroxyl group aligned along the bilayer normal induces lipid ordering and increases bilayer thickness.^{42,43} On the other hand, a large, anisotropic, but flexible fluorescent molecule (diphenyl-hexatriene)⁴⁴ adopts a range of orientations within the bilayer, leading to no effect on the bilayer thickness. Among small molecules, hexane partitions completely to the low-density bilayer center region,⁴⁵ leading to no effect on bilayer thickness. Small aliphatic alcohols, on the other hand, partition into the high-density lipid headgroup region and affect bilayer packing, leading to a reduction in bilayer thickness.⁴⁶ Ibuprofen in its charged form is analogous to small aliphatic alcohols and partitions into the polar region of the bilayer, intercalating between the phospholipid headgroups. This disrupts the bilayer packing and leads to a membrane area expansion while preserving the volume of the hydrocarbon region. Ibuprofen in its uncharged form partitions into the hydrocarbon region,¹⁴ perhaps due to its nonpolar hydrophobic nature. Our MD simulations indicated that the headgroup region was significantly perturbed and, as shown in Figure 8 via the distance between headgroup atoms of two lipid monolayers, it is possible to infer that this local disruption of bilayer structure

resulted in the reduction of bilayer thickness. Overall, diffraction and MD simulations indicate that ibuprofen partitions into the bilayer irrespective of the drug charge state. However, the peak location of the drug distribution is in either the headgroup or the tail regions of the bilayer depending on the charge state of the drug and is consistent with previous studies of other membrane-active molecules.

The changes in headgroup hydration caused by ibuprofen incorporation are consistent with the observations for other lipid membrane-active solutes. For example, cholesterol decreases water penetration into the bilayer headgroup by ≈ 2.5 Å (at cholesterol/lipid ratios of 1/2),⁴⁷ whereas some peptides change the water penetration depending on the pH⁴⁸ or slightly increase the number of water molecules/lipid.⁴⁹ Short chain alcohols are localized to the headgroup region of the lipid and affect the headgroup hydration.^{46,50} As found in this study, the presence of ibuprofen increases the number of water molecules per lipid (N_w) with increasing D/L ratio. Radial distribution functions (RDF) calculated using MD simulations revealed the significant hydration of drug in charged form (as applicable to diffraction experiments) within the bilayer as plausible reason for this increase (Figure 7b). However, MD simulations predicted that the drug in uncharged form is likely to stay unhydrated within the bilayer. Also, the hydration of lipid headgroup moieties is unaffected (Figure 7a) and remains unchanged due to the addition of drug irrespective of the drug charge state.

CONCLUSIONS

In contrast to other studies that rely heavily on molecular tags and indirect methods to probe interactions of NSAIDs with lipid membranes, the present study offers a more accurate picture of the ibuprofen–lipid bilayer system drawn from neutron diffraction measurements in conjunction with all-atom MD simulations. Isomorphous replacement of hydrogen with deuterium was used as a nonperturbing label for determining the position and distribution of the drug and water molecules along the bilayer normal. One-dimensional distribution of matter at neutral pH (when the drug is likely to carry a charge of -1) was thus determined by neutron diffraction and found to agree with predictions from MD simulations. Using neutron diffraction, charged ibuprofen molecules were found to reside at the interface between the polar lipid headgroup and the hydrocarbon regions of the bilayer. Their presence in the bilayer causes bilayer thinning and increases membrane hydration. MD simulations further revealed that this increase in hydration was due to the drug molecules being hydrated in the bilayer by a few water molecules while leaving the lipid headgroup hydration intact. MD predictions were further extended to the uncharged form of the drug, found at low pH, to reveal that drug locates within the bilayer slightly deeper than the charged form.

The fact that ibuprofen dissolves readily into the lipid bilayer even at high concentrations and affects the local bilayer structure supports the hypothesis that topical interactions between NSAIDs and lipid lining of the GI tract might have a contributory effect on NSAID-induced GI toxicity. Moreover, strong interactions between ibuprofen and PC lipids suggest that NSAIDs could be good candidates for liposome-based drug delivery. Such delivery systems would not only enhance the drug solubility in formulations but also allow for targeted delivery of NSAIDs to the sites of inflammation while avoiding direct topical interactions with the stomach lining. Finally, we

note that ibuprofen is a smaller molecule among variety of other NSAIDs with bulkier hydrophobic groups with some even exhibiting complex charge states. However, due to the amphiphilic nature of most NSAIDs, all of them are likely to partition into the bilayer irrespective of the drug charge state, and perturb the bilayer structure in a similar way.

MATERIALS AND METHODS

Neutron Diffraction Experiments and Data Treatment. Data treatment and analysis followed procedures described previously.^{28,31,33–35} Briefly, experiments were performed using the Advanced Neutron Diffractometer/Reflectometer at the National Institute of Standards and Technology Center for Neutron Research (Gaithersburg, MD) using neutron beam of $\lambda = 5$ Å. Multilamellar samples were prepared by depositing dispersion of DOPC (Avanti Polar Lipids Inc. (Alabaster, AL) and used without further purification) or ibuprofen (Sigma Aldrich)–DOPC mixtures (D/L ratios of 0/1, 1/5, 1/4, 1/3, and 1/2) codissolved in chloroform on a microscope glass slide drop-by-drop, vacuum-dried at room temperature, and equilibrated overnight in the vapor of a saturated salt (NaCl) solution, prior to the experiments. The relative humidity was maintained at 86% and the temperature of 23 °C throughout the measurements. For each D/L ratio, two samples were prepared, one with protonated ibuprofen (H-IBU) and another with deuterated ibuprofen (α -CD3 or D-IBU) containing three deuterium atoms as label attached to the α -carbon next to the carboxylic group of the drug. This allowed determining the position and drug distribution by deuterium contrast. Each sample (composition) was hydrated and measured under a few different H_2O/D_2O contrast conditions ($\xi = D_2O/H_2O$: 0, 0.16, or 0.20 and 0.5) for determining phases of the structure factors (see below) as well as the water distribution. Repeated scans were collected to make sure that the equilibration of the lipid samples with the humid vapor was reached. Scans were visualized, and averaged using the software package *refred*,⁵¹ which were then processed independently for the determination of the scattering length density on an absolute-relative scale. The structure factors were determined as the square root of integrated Bragg peak intensity with some corrections, as given by $f(h) = (I(h)A(h) \sin(2\theta^*))^{1/2}$. $I(h)$ is the area under diffraction peak of order h after background subtraction, $\sin(2\theta^*)$ is the Lorentz correction factor, and $A(h)$ is the absorption coefficient (3). Structure factors (on an arbitrary scale) were then used to calculate the absolute scattering length density (SLD) $\rho(z)$ along the bilayer normal given by

$$\rho(z) = \rho_0 + \left(\frac{2}{d}\right) \sum_{h=1}^{h_{\text{obs}}} kf(h) \cos\left[\frac{2\pi hz}{d}\right] \quad (1)$$

where k is the instrumental constant, $h_{\text{obs}} (=5)$ is the maximum observed diffraction peaks, d is the Bragg spacing, and ρ_0 is the average SLD of the unit cell. The above $\rho(z)$ profile is per volume of the unit cell, which contains two lipid molecules of each monolayer and associated water molecules. It was placed on an internally consistent absolute scale on a per-lipid basis^{28,31} by multiplying $\rho(z)$ with the area/lipid S (volume/unit cell = $S \times d$) given by

$$\rho^*(z) = \rho(z)S = \rho_0^* + \left(\frac{2}{d}\right) \sum_{h=1}^{h_{\text{obs}}} kf(h) \cos\left[\frac{2\pi hz}{d}\right] \quad (2)$$

The average scattering length/length of the unit cell (ρ_0^*) in eq 2 is given by

$$\begin{aligned} \rho_0^* &= (2/d)(N_w(\xi b_{D_2O} + (1 - \xi)b_{H_2O}) + (1 - \chi_{\text{drug}})b_{\text{lipid}} \\ &\quad + \chi_{\text{drug}}(b_{D\text{-IBU}} - b_{H\text{-IBU}})) \\ &= (2/d)(N_w(\xi b_{D_2O} + (1 - \xi)b_{H_2O}) + (1 - \chi_{\text{drug}})b_{\text{lipid}} \\ &\quad - \chi_{\text{drug}}b_{H\text{-IBU}} + \chi_{\text{drug}}n_D(b_D - b_H)) \end{aligned} \quad (3)$$

where N_w is the number of waters/lipid, b_{D_2O}/b_{H_2O} , b_{lipid} , b_{D-drug}/b_{H-drug} , and b_D/b_H are the scattering lengths of deuterated/protonated water, lipid, drug, and deuterium/hydrogen, respectively, while χ_{drug} is the drug molar fraction (or per half unit cell) and $n_D(=3)$ is the number of deuterium atoms in D-IBU. The drug/water distributions can be described by single Gaussian distributions. We then used the single Gaussian model to extract the scale factors k_ξ^D and k_ξ^H for different drug molar fractions (χ_{drug}) by model fitting of the difference structure as in eq 5 below.^{33,34} The difference SLD of two samples with D-IBU and H-IBU can be written as

$$\Delta\rho^*(z) = \left(\frac{\chi_{drug} n_D (b_D - b_H)}{A_{drug} \sqrt{\pi}} \right) \left(\exp \left[- \left(\frac{z - z_{drug}}{A_{drug}} \right)^2 \right] + \exp \left[- \left(\frac{z + z_{drug}}{A_{drug}} \right)^2 \right] \right) \quad (4)$$

where z_{drug} and A_{drug} are the peak position and 1/e-halfwidth of drug distribution. The Fourier transform of eq 4 leads to

$$F_\chi^D(h) - F_\chi^H(h) = k_\chi^D f_\chi^D(h) - k_\chi^H f_\chi^H(h) \\ = 2\chi_{drug} n_D (b_D - b_H) \exp \left[- \left(\frac{\pi A_{drug} h}{d} \right)^2 \right] \cos \left[\frac{2\pi h z_{drug}}{d} \right] \quad (5)$$

from which scaling factors and drug distribution parameters z_{drug} and A_{drug} were determined. All SLD profiles for a given sample composition (χ_{drug}), measured in different H_2O/D_2O vapor conditions (ξ), will be scaled by one scale factor (k) determined above. The difference between scaled structure factor, for a given sample measured in H_2O ($\xi = 0$) or a H_2O/D_2O ($\xi > 0$) vapor mixture, respectively, can be used to determine the water peak and the number of water molecules per half unit cell (N_w) using eq 6 given by

$$F_\xi(h) - F_0(h) = k_\xi (f_\xi(h) - f_0(h)) \\ = 2\xi N_w (b_{D_2O} - b_{H_2O}) \exp \left[- \left(\frac{\pi A_{water} h}{d} \right)^2 \right] \cos \left[\frac{2\pi h z_{water}}{d} \right] \quad (6)$$

The parameter z_{water} was fixed at $d/2$ leaving only A_{water} as the fitting parameter. In the case of pure DOPC, N_w was set to 7.7 for 86% relative humidity.³³ For the other compositions (χ), N_w was determined via eq 6, using the drug (D3) peak for calibration of the absolute scale of SLD.³⁴ Phase determination of the structure factors was done using a few H_2O/D_2O contrasts and eq 6.

All terms on the right-hand side of eq 6 are positive-definite, except that of the cosine term, which depends on h and z_{water} and determines the signs of the structure factors. Setting $z_{water} = d/2$ results in the cosine term being -1 ($+1$) when h is odd (even).⁵² Signs of the structure factors were chosen such that the slope of f_ξ versus ξ was consistent with the sign predicted by the cosine term. The mean and standard errors in drug distribution profiles were obtained using Monte Carlo error analysis^{28,31} where errors from raw data and from the scaled structure factors were used to generate 100 synthetic scattering length density profiles. Each of these synthetic data sets was then used for the determination of scale factors, drug, and water distribution parameters.

Molecular Dynamics Simulations. Simulations were performed using the GROMACS 3.3.3 package.³⁶ The initial structure of well-equilibrated bilayer contained 128 DOPC lipids and 4789 water molecules.⁵³ The lipid molecules were modeled on the basis of Berger et al.³⁷ and the *ffgmx* as implemented in GROMACS, both based on GROMOS87 with improvements. Water molecules were modeled using the SPC model,³⁴ and NSAID molecules were modeled using PRODRG.³⁸ Integration based on a leapfrog algorithm with a time step of 2 fs was used. Lennard-Jones (LJ) potential was switched at 1.0 nm to go smoothly to zero at 1.2 nm. Electrostatic interactions were

computed using a Particle-Mesh Ewald (PME) sum⁵⁵ with a direct space cutoff at 1.4 nm and fast-Fourier grid space of 0.12 nm with fourth-order interpolation and a tolerance of 10^{-5} . Short-range LJ and the electrostatic interactions were accounted for by maintaining a neighbor list over 1.4 nm, updated every 50 fs. The pressure (coupling constant of 1 ps) was maintained at 1 bar, and the temperature (coupling constant of 0.1 ps) was maintained at 296 K.⁵⁶ The trajectory was saved every 10 ps. VMD software⁵⁷ was used for visualization and for drug insertion to create initial structures. We simulated five systems: DOPC and ibuprofen (charged and neutral)/DOPC at mole ratios of 1/4 and 1/2. NSAID molecules were placed within the lipid bilayer in eight layers separated along the bilayer normal and in a more or less lattice position to avoid drug clusters in the starting configuration (Figure 6a). The total length of each run was 35.1 ns. Equilibration was established by observing the number of system parameters (e.g., potential energy, headgroup area). The drug distribution was unchanged after the initial 15.1 ns, and all of the analyses were done using the last 20 ns of the data. The number densities for each element in the simulation system were first calculated by binning the bilayer into 200 bins (width ≈ 0.4 Å) and then multiplying by the respective scattering lengths to give the final scattering length density (SLD) profiles. Other methods of estimating SLD profiles, using Fermi width (~ 1 Å) for each atom center,⁵⁸ discrete Fourier structure factors,⁵⁹ or Gaussian distributions located at atomic nuclei,⁶⁰ have been shown to be equivalent with only minor differences for comparison between MD and neutron diffraction.

■ ASSOCIATED CONTENT

📄 Supporting Information

Additional insights exclusively obtained using MD simulations provided as figures. This material is available free of charge via the Internet at <http://pubs.acs.org>.

■ AUTHOR INFORMATION

Corresponding Author

ramanan@uh.edu

Present Address

^{||}Rensselaer Polytechnic Institute, 110 Eighth Street, Troy, New York 12180, United States.

Notes

The authors declare no competing financial interest.

■ ACKNOWLEDGMENTS

We thank the Texas Higher Education Coordinating Board through the Advanced Technology Program for partial financial support of this work. We also thank the National Science Foundation (grant no. CMMI-0708096) for partial financial support. We acknowledge the Texas Learning & Computation Center at the University of Houston for the computational resources. We also thank Assistant Professor Manolis Doxastakis (University of Houston) and Professor Lenard M. Lichtenberger (The University of Texas Health Science Center at Houston) for their useful comments of the manuscript.

■ REFERENCES

- (1) Donnelly, M. T.; Hawkey, C. J. *Aliment. Pharmacol. Ther.* **1997**, *11*, 227–236.
- (2) Thun, M. J.; Henley, S. J.; Patrono, C. J. *Natl. Cancer Inst.* **2002**, *94*, 252–266.
- (3) Weggen, S.; Eriksen, J. L.; Das, P.; Sagi, S. A.; Wang, R.; Pietrzik, C. U.; Findlay, K. A.; Smith, T. E.; Murphy, M. P.; Bulter, T. *Nature* **2001**, *414*, 212–216.
- (4) Lichtenberger, L. M.; Wang, Z. M.; Romero, J. J.; Ulloa, C.; Perez, J. C.; Giraud, M. N.; Barreto, J. C. *Nat. Med.* **1995**, *1*, 154–158.
- (5) Vane, J. R. *Nature* **1971**, *231*, 232–235.
- (6) Lichtenberger, L. M. *Biochem. Pharmacol.* **2001**, *61*, 631–637.

- (7) Wallace, J. L.; Soldato, P. D. *Fundam. Clin. Pharmacol.* **2003**, *17*, 11–20.
- (8) Zhou, Y.; Plowman, S. J.; Lichtenberger, L. M.; Hancock, J. F. *J. Biol. Chem.* **2010**, *285*, 35188–35195.
- (9) Barbato, F.; LaRotonda, M. I.; Quaglia, F. *J. Pharm. Sci.* **1997**, *86*, 225–229.
- (10) Lichtenberger, L. M.; Zhou, Y.; Jayaraman, V.; Doyen, J. R.; O'Neil, R. G.; Dial, E. J.; Volk, D. E.; Gorenstein, D. G.; Boggara, M. B.; Krishnamoorti, R. *Biochim. Biophys. Acta, Mol. Cell Biol. Lipids* **2012**, *1821*, 994–1002.
- (11) Gordeliy, V. I.; Chernov, N. I. *Acta Crystallogr., Sect. D* **1997**, *53*, 377–384.
- (12) Boggara, M. B.; Faraone, A.; Krishnamoorti, R. *J. Phys. Chem. B* **2010**, *114*, 8061–8066.
- (13) Boggara, M. B.; Krishnamoorti, R. *Langmuir* **2010**, *26*, 5734–5745.
- (14) Boggara, M. B.; Krishnamoorti, R. *Biophys. J.* **2010**, *98*, 586–595.
- (15) Ferreira, H.; Lúcio, M.; Lima, J.; Matos, C.; Reis, S. *Anal. Bioanal. Chem.* **2005**, *382*, 1256–1264.
- (16) Chakraborty, H.; Mondal, S.; Sarkar, M. *Biophys. Chem.* **2008**, *137*, 28–34.
- (17) Tomisato, W.; Tanaka, K.; Katsu, T.; Kakuta, H.; Sasaki, K.; Tsutsumi, S.; Hoshino, T.; Aburaya, M.; Li, D. W.; Tsuchiya, T.; Suzuki, K.; Yokomizo, K.; Mizushima, T. *Biochem. Biophys. Res. Commun.* **2004**, *323*, 1032–1039.
- (18) Mondal, S.; Sarkar, M. *Langmuir* **2011**, *27*, 15054–15064.
- (19) Hüsch, J.; Dutagaci, B.; Glaubitz, C.; Geppert, T.; Schneider, G.; Harms, M.; Müller-Goymann, C. C.; Fink, L.; Schmidt, M. U.; Setzer, C.; Zirkel, J.; Rebmann, H.; Schubert-Zsilavec, M.; Abdel-Tawab, M. *Eur. J. Pharm. Sci.* **2011**, *44*, 103–116.
- (20) Nunes, C.; Brezesinski, G.; Pereira-Leite, C.; Lima, J. L. F. C.; Reis, S.; Lúcio, M. *Langmuir* **2011**, *27*, 10847–10858.
- (21) Nunes, C.; Brezesinski, G.; Lima, J. L. F. C.; Reis, S.; Lúcio, M. *J. Phys. Chem. B* **2011**, *115*, 8024–8032.
- (22) Roy, S. M.; Bansode, A. S.; Sarkar, M. *Langmuir* **2010**, *26*, 18967–18975.
- (23) Manrique-Moreno, M.; Suwalsky, M.; Villena, F.; Garidel, P. *Biophys. Chem.* **2010**, *147*, 53–58.
- (24) Zhou, Y.; Hancock, J. F.; Lichtenberger, L. M. *PLoS One* **2010**, *5*, e8811.
- (25) Moreno, M. M.; Garidel, P.; Suwalsky, M.; Howe, J.; Brandenburg, K. *Biochim. Biophys. Acta, Biomembr.* **2009**, *1788*, 1296–1303.
- (26) Lúcio, M.; Ferreira, H.; Lima, J. L. F. C.; Reis, S. *Redox Rep.* **2008**, *13*, 225–236.
- (27) Sousa, C.; Nunes, C.; Lúcio, M.; Ferreira, H.; Lima, J. L. F. C.; Tavares, J.; Cordeiro-Da-Silva, A.; Reis, S. *J. Pharm. Sci.* **2008**, *97*, 3195–3206.
- (28) Wiener, M. C.; White, S. H. *Biophys. J.* **1991**, *59*, 162–173.
- (29) King, G. I.; White, S. H. *Biophys. J.* **1986**, *49*, 1047–1054.
- (30) Büldt, G.; Gally, H. U.; Seelig, A.; Seelig, J. *Nature* **1978**, *271*, 182–184.
- (31) Wiener, M. C.; White, S. H. *Biophys. J.* **1991**, *59*, 174–185.
- (32) Wiener, M. C.; King, G. I.; White, S. H. *Biophys. J.* **1991**, *60*, 568–576.
- (33) Hristova, K.; White, S. H. *Biophys. J.* **1998**, *74*, 2419–2433.
- (34) Krepkij, D.; Mihailescu, M.; Freites, J. A.; Schow, E. V.; Worcester, D. L.; Gawrisch, K.; Tobias, D. J.; White, S. H.; Swartz, K. *J. Nature* **2009**, *462*, 473–479.
- (35) Mihailescu, M.; Vaswani, R. G.; Jardon-Valadez, E.; Castro-Roman, F.; Freites, J. A.; Worcester, D. L.; Chamberlin, A. R.; Tobias, D. J.; White, S. H. *Biophys. J.* **2011**, *100*, 1455–1462.
- (36) Lindahl, E.; Hess, B.; van der Spoel, D. *J. Mol. Model.* **2001**, *7*, 306–317.
- (37) Berger, O.; Edholm, O.; Jähnig, F. *Biophys. J.* **1997**, *72*, 2002–2013.
- (38) Schüttelkopf, A. W.; van Aalten, D. M. F. *Acta Crystallogr., Sect. D* **2004**, *60*, 1355–1363.
- (39) Marrink, S.-J.; Berendsen, H. J. C. *J. Phys. Chem.* **1994**, *98*, 4155–4168.
- (40) Chakraborty, H.; Banerjee, R.; Sarkar, M. *Biophys. Chem.* **2003**, *104*, 315–325.
- (41) Ferreira, H.; Lúcio, M.; de Castro, B.; Gameiro, P.; Lima, J.; Reis, S. *Anal. Bioanal. Chem.* **2003**, *377*, 293–298.
- (42) Pencer, J.; Nieh, M. P.; Harroun, T. A.; Krueger, S.; Adams, C.; Katsaras, J. *Biochim. Biophys. Acta, Biomembr.* **2005**, *1720*, 84–91.
- (43) Róg, T.; Pasenkiewicz-Gierula, M.; Vattulainen, I.; Karttunen, M. *Biochim. Biophys. Acta, Biomembr.* **2009**, *1788*, 97–121.
- (44) Pebay-Peyroula, E.; Dufourc, E. J.; Szabo, A. G. *Biophys. Chem.* **1994**, *53*, 45–56.
- (45) White, S. H.; King, G. I.; Cain, J. E. *Nature* **1981**, *290*, 161–163.
- (46) Ly, H. V.; Longo, M. L. *Biophys. J.* **2004**, *87*, 1013–1033.
- (47) Simon, S. A.; McIntosh, T. J.; Latorre, R. *Science* **1982**, *216*, 65–67.
- (48) Bradshaw, J. P.; Dempsey, C. E.; Watts, A. *Mol. Membr. Biol.* **1994**, *11*, 79–86.
- (49) Hristova, K.; Wimley, W. C.; Mishra, V. K.; Anantharamiah, G. M.; Segrest, J. P.; White, S. H. *J. Mol. Biol.* **1999**, *290*, 99–117.
- (50) Pillman, H. A.; Blanchard, G. J. *J. Phys. Chem. B* **2010**, *114*, 3840–3846.
- (51) Kienzle, P. A.; O'Donovan, K. V.; Ankner, J. F.; Berk, N. F.; Majkrzak, C. F. 2000–2006; <http://www.ncnr.nist.gov/reflpak>.
- (52) Zaccai, G.; Blasie, J. K.; Schoenborn, B. P. *Proc. Natl. Acad. Sci. U.S.A.* **1975**, *72*, 376–380.
- (53) Shirley, W. I. S.; Robert, V.; Pavel, J.; Rainer, A. B. *J. Chem. Phys.* **2008**, *128*, 125103.
- (54) Berendsen, H. J. C.; Postma, J. P. M.; van Gunsteren, W. F.; Hermans, J. In *Intermolecular Forces*; Pullman, B., Ed.; Reidel: Dordrecht, 1981; pp 331–342.
- (55) Essmann, U.; Perera, L.; Berkowitz, M. L.; Darden, T.; Lee, H.; Pedersen, L. G. *J. Chem. Phys.* **1995**, *103*, 8577–8593.
- (56) Berendsen, H. J. C.; Postma, J. P. M.; van Gunsteren, W. F.; DiNola, A.; Haak, J. R. *J. Chem. Phys.* **1984**, *81*, 3684.
- (57) Humphrey, W.; Dalke, A.; Schulten, K. *J. Mol. Graphics* **1996**, *14*, 33–38.
- (58) Léonard, A.; Escribe, C.; Laguerre, M.; Pebay-Peyroula, E.; Neri, W.; Pott, T.; Katsaras, J.; Dufourc, E. J. *Langmuir* **2001**, *17*, 2019–2030.
- (59) Benz, R. W.; Castro-Román, F.; Tobias, D. J.; White, S. H. *Biophys. J.* **2005**, *88*, 805–817.
- (60) Tu, K.; Tobias, D. J.; Klein, M. L. *Biophys. J.* **1995**, *69*, 2558–2562.